Macromolecules
ARTICLE

Macromolecules **2009**, *42*, 4993–5000 **4993**
DOI: 10.1021/ma900749v

Controlled Radical Synthesis of Fluorene-Based Blue-Light-Emitting Copolymer Nanospheres with Core−Shell Structure via Self-Assembly

Rui Wang, Wei-Zhi Wang, Su Lu, and Tianxi Liu*

Key Laboratory of Molecular Engineering of Polymers of Ministry of Education, Department of Macromolecular Science, Laboratory of Advanced Materials, Fudan University, Shanghai 200433, China

Received April 7, 2009; Revised Manuscript Received May 8, 2009

ABSTRACT: We prepared a series of well-defined polyfluorene-based copolymers by using polyfluorene (PF) macroinitiators to initiate atom transfer radical polymerization (ATRP) of γ-methacryloxypropyltrimethoxysilane (MPS). The chemical structures of hydroxy-functionalized PF (PFOH), PF macroinitiators (PFBr), and polyfluorene-*b*-poly(γ-methacryloxypropyltrimethoxysilane) (PF-*b*-PMPS) block copolymers were confirmed by ^{1}H NMR. In THF/aqueous solution, amphiphilic PF-*b*-PMPS block copolymers can self-assemble into core−shell micelles with PMPS as the core and PF as the shell. Base-catalyzed sol−gel process inside the PMPS core results in PF-encapsulated silica core−shell nanospheres. Transmission electron microscopy (TEM) studies reveal the dense grafting of PF on the surface of silica core. The effect of PF-*b*-PMPS core−shell structures on the optical and electrochemical properties was also investigated. This novel kind of luminescent nanosphere has potential applications in bioanalysis, biomedical, and light-emitting devices.

Introduction

Organic/inorganic hybrid nanomaterials have attracted considerable interest in the past decade because of the fascinating size-dependent optical, magnetic, and electronic properties of particles on the nanoscale.[1−3] It is well known that amphiphilic block copolymers can self-assemble into aggregates with various morphologies in water. Starting from a trimethoxysilyl-containing monomer, Chen et al. have synthesized poly(ethylene oxide)-*b*-poly(γ-methacryloxypropyltrimethoxysilane) (PEO-*b*-PMPS) by atom transfer radical polymerization (ATRP), and the PEO-*b*-PMPS block copolymers could form vesicles or micelles depending on the relative block length and preparation conditions.[4−6] Liu et al. also fabricated nanoparticles with different characters and functions via self-assembly of block copolymers contained PMPS block in aqueous solution.[7] The organic polymer shell determines the chemical properties of nanoparticles, the interaction with the environments, and their responsiveness to external stimuli.

Microspheres containing chromophores have been utilized in an extensive variety of applications. In the literature, semiconductor nanocrystals are used as the chromophores.[8−13] Semiconductor nanocrystals or quantum dots are promising candidates for use as active components in materials for both biotechnology and nanoelectronics. Properties such as narrow luminescence profiles over a broad excitation range are critical for nanoparticle-based devices including biological probes,[13] light-emitting diode displays,[14] tunable lasers, and photovoltaic cells.[10] Photonic nanocrystals are a kind of heavy metal compound, such as Cd/Te,[8,9] Cd/Se,[10,11] and CdSe/ZnS;[12,13] metal nanoparticles, such as Au nanoparticles,[3] are usually utilized as the chromophores of the luminescent nanomaterials. Actually, the polymers, which are usually used to coat or stabilize the photonic nanocrystals, do not have self-luminescence ability. Therefore, the use of luminescent polymers may be a simple but efficient method for fabricating luminescent nano- or microspheres.

*Corresponding author. Tel: +86-21-5566 4197. Fax: +86-21-6564 0293. E-mail: txliu@fudan.edu.cn.

Conjugated (semiconducting) polymers are a novel class of materials that combine the optical and electronic properties of semiconductors with the processing advantages and mechanical properties of polymers.[15] This kind of polymers has both photoluminescence (PL) and electroluminescence abilities that distinctly differ from those of traditional polymers. Although conjugated polymers are widely used to fabricate light-emitting diodes, to our knowledge, little work has been reported on the synthesis of luminescent nanospheres or microspheres based on conjugated block polymers by self-assembly.

Polyfluorene as a kind of blue-light-emitting conjugated polymers is one of the most promising materials for light-emitting diodes because of its thermal stability and high efficiency for both PL and electroluminescence. Fluorene contains a rigid planar biphenyl unit, and the substituent derivatives at the C-9 position of the monomeric fluorene offer the prospect of controlling polymer properties such as solubility, emission wavelengths, processability, and potential interchain interactions in films.[16] Polyfluorene was usually used as a thin film in light-emitting devices, and so far, the nanosphere-contained polyfluorenes have not yet been reported. In this work, we have found a novel approach for obtaining nanospheres based on polyfluorene.

Recently, we have synthesized polyfluorene-based light-emitting rod−coil block copolymers by ATRP.[17−19] In this work, we used a similar approach to synthesize polyfluorene-*b*-poly(γ-methacryloxypropyltrimethoxysilane) (PF-*b*-PMPS) rod−coil block copolymers. The amphiphilic PF-*b*-PMPS could self-assemble into micelles with PMPS core and PF shell in THF/H_2O solution. The base-catalyzed sol−gel process inside the PMPS core induces the formation of PF-encapsulated hybrid core−shell nanospheres. These blue-light-emitting nanospheres based on polyfluorene show spherical configuration and well-defined core−shell structure, and importantly, still retained good luminescence ability because of the special luminescence properties of polyfluorene.

Published on Web 05/29/2009

Experimental Part

All reactions were carried out under a nitrogen atmosphere. Solvents were used as received commercially. ^{1}H NMR and ^{13}C NMR spectra were recorded using Varian Mercury plus 400 spectrometers, and chemical shifts were reported in ppm units with tetramethylsilane as an internal standard. Chloroform ($CDCl_3$) was mainly used as the solvent for recording NMR spectra. Molecular weights and polydispersities of the polymers were determined by gel permeation chromatography (GPC) analysis with polystyrene as the standard. The mobile phase was THF flowing at 1.0 mL/min. Elemental analyses were performed on a Vario EL elemental analysis instrument (Elementar). The polymer samples were analyzed by Voyager DE-STR matrix-assisted laser desorption ionization time-of-flight mass spectrometry (MALDI-TOF). Transmission electron microscopy (TEM) observation was performed with a Philips CM300 FEG TEM instrument operated under an acceleration voltage of 300 kV. Cyclic voltammetry (CV) was carried out on a T30/FRA2 electrochemical workstation with a standard three-electrode electrochemical cell at a scan rate of 50 mV/s with nitrogen-saturated solution of 0.10 M tetrabutylammonium hexafluorophosphate (Bu_4NPF_6) in acetonitrile (CH_3CN). UV−visible absorption spectra were obtained on a Shimadzu UV-3150 spectrophotometer. The PL spectra were recorded on a Shimadzu RF-5301 PC fluorometer at room temperature.

Synthesis of 2,7-Dibromo-9,9-dioctylfluorene. Fluorene (10 g) and potassium hydroxide (33.6 g) were mixed together and protected by nitrogen, and then DMSO (100 mL) was added using an injector. The mixture was stirred for 15 min at room temperature to dissolve the fluorene completely. After the addition of 1-bromooctane (25.5 mL) by injector, the mixture was stirred for at least 24 h below 30 °C. After being extracted by petroleum ether and purified through chromatographic column, 9,9-dioctylfluorene (white crystal) was obtained with a yield of 78%. To a solution of 9,9-dioctylfluorene in chloroform (60 mL) at 0 °C were added ferric chloride (0.15 g) and bromine (6.44 mL) to a two-mouth flask. The flask was packed by aluminum foil to avoid light. After being stirred for 4 h, the solution of sodium hydrosulfite was added until the color of bromine disappeared. The mixture was washed by water and extracted by chloroform and then purified through chromatographic column and recrystallized from ethanol. 2,7-Dibromo-9,9-dioctylfluorene (white crystal) was obtained in 80% yield. ^{1}H NMR (400 MHz, $CDCl_3$, δ): 7.53 (d, 2H), 7.46 (d, 2H), 7.44 (d, 2H), 1.91 (m, 4H), 1.26−1.05 (m, 20H), 0.83 (t, 6H), 0.58 (m, 4H). ^{13}C NMR (133 MHz, $CDCl_3$, δ): 152.44, 138.94, 130.04, 126.07, 121.38, 120.96, 55.56, 40.02, 31.63, 29.78, 29.04, 29.01, 23.51, 22.47, 13.94. HRMS: calcd for $C_{29}H_{40}Br_2$, 546.150; found, 546.149.

Synthesis of 9,9-Dioctyl-2-bromo-7-4,4,5,5-tetramethyl-1,3,2-dioxaborolan-2-yl Fluorene. *n*-Butyllithium (5 mL, 8 mmol, 1.6 M in hexane) was added dropwise to a solution of 2,7-dibromo-9,9-dioctylfluorene (4.38 g, 8 mmol) in THF (30 mL) at −78 °C. The mixture was stirred at −78 °C for 1 h, and 8 mmol of 2-isopropoxy-4,4,5,5-tetramethyl-1,3,2-dioxaborolane was rapidly added to the mixture. The solution was stirred at −78 °C for another 1 h, then warmed to room temperature and stirred for 20 h, and finally purified through a chromatographic column by petroleum ether. ^{1}H NMR (400 MHz, $CDCl_3$, δ): 7.80, 7.65, 7.57, 7.45 (d, fluorene aromatic protons), 7.72, 7.26 (s, fluorene aromatic protons), 1.90−1.99 (br, $-CH_2C_7H_{15}$), 1.25−0.80 (m, $-CH_2C_7H_{15}$). ^{13}C NMR (133 MHz, $CDCl_3$, δ): 150.35, 143.75, 133.44, 128.74, 119.25, 83.57, 55.13, 39.38, 31.55, 29.81, 29.06, 29.01, 24.79, 23.42, 22.45, 13.91. HRMS: calcd for $C_{35}H_{52}BBrO_2$, 594.32; found, 594.26.

Synthesis of Phenylboronic Acid. *n*-Butyllithium (2 mL, 3.2 mmol, 1.6 M in hexane) was added dropwise to a solution of bromobenzene (4.71 g, 3 mmol) in THF (30 mL) at −78 °C. The mixture was stirred at −78 °C for 1 h, and 3.2 mmol trimethyl borate was rapidly added to the mixture. The solution was stirred at −78 °C for another 1 h and then warmed to room temperature and stirred for 20 h. Superfluous HCl (2 M) was allowed to be added to the solution, and the solution was stirred for 1 h. The mixture solution was extracted with CH_2Cl_2 and water. Then, CH_2Cl_2 was concentrated and poured in petroleum ether to obtain a white crystal of about 0.5 g. Anal. Calcd for [$C_6H_7BO_2$]: C, 59.10; H, 5.79. Found: C, 59.12; H, 5.81.

Polymerization of Hydroxy-Functionalized Polyfluorene (PFOH). The general procedure of polymerization was carried out through the Suzuki coupling reaction. 9,9-Dioctyl-2-bromo-7-4,4,5,5-tetramethyl-1,3,2-dioxaborolan-2-yl fluorene (3 mmol, 1.475 g) and $Pd(PPh_3)_4$ (1.0 mol %) were put in a 50 mL flask. Then, a mixture of toluene and 2 M K_2CO_3(aq) (3:2 v/v) was added. The mixture was vigorously stirred at 85−90 °C for 4 h under the protection of nitrogen, and then 4-bromobenzyl alcohol (0.3 mmol, 0.056 g) was added to the flask. After stirring for 64 h at 85−90 °C, phenylboronic acid (0.3 mmol, 0.036 g) was added. After another 4 h, the mixture was cooled to room temperature and then filtrated in methanol and desiccated in vacuum. ^{1}H NMR (400 MHz, $CDCl_3$, δ): 7.85 −7.65 (br, fluorene aromatic protons), 7.50, 7.35 (2d, phenyl end groups), 4.78 (s, PhCH_2O−), 2.12 (br, $-CH_2C_7H_{15}$), 1.25−0.80 (m, $-CH_2C_7H_{15}$). M_n: 5000 and M_w: 9000.

Synthesis of Polyfluorene Macroinitiators. PFOH (0.9 g, 0.18 mmol), triethylamine (TEA, 1.4 mL, 10 mmol), and dry CH_2Cl_2 (20 mL) were placed in a 100 mL round-bottomed flask. After cooling to 0 °C, 2-bromoisobutyryl bromide (1.2 mL, 8 mmol) was added dropwise with vigorous stirring under an argon atmosphere. The temperature was allowed to rise to 20 °C, and the reaction mixture was stirred overnight. The solution was extracted with water to remove the salt and the excess of bromoisobutyryl bromide. After being dried over anhydrous sodium sulfate, the clear solution was concentrated, and bromo-ended PF macroinitiator was precipitated in methanol. After filtration, the solid was dried under vacuum at 40 °C, and 0.88 g of faint yellow product was obtained (95% in yield).^{1}H NMR (400 MHz, $CDCl_3$, δ): 7.85−7.65 (br, ring aromatic protons), 7.50, 7.35 (2 d, phenyl end groups), 5.29 (s, Ph−CH_2O−), 2.12 (br, $-CH_2C_7H_{15}$), 1.99 (s, $-C(CH_3)_2Br$), 1.25−0.80 (m, $-CH_2C_7H_{15}$).

Synthesis of Polyfluorene-*b*-poly(γ-methacryloxypropyltrimethoxysilane) (PF-*b*-PMPS) Block Copolymers by Atom Transfer Radical Polymerization. In a typical run, a glass tube was charged with 0.05 g (0.01 mmol) of PF macroinitiator, 2.8 mg (0.02 mmol) of CuBr, determinate amount of methacryloxypropyltrimethoxysilane (MPS), and 0.80 mL of *o*-dichlorobenzene (ODCB) before it was sealed with a rubber septum. After being degassed by three freeze−pump−thaw cycles, the glass reactor was immersed in an oil bath at 90 °C, and 1,1,4,7,10,10-hexamethyltriethylenetetramine (HMTETA) (5.4 μL, 0.02 mmol) was added with syringes. A clear solution of a light-green color was formed within a few minutes. After 10 h, the product was precipitated in methanol (40 mg). ^{1}H NMR (400 MHz, $CDCl_3$, δ): 7.83−7.67 (br, fluorene aromatic protons), 7.50−7.40 (br, phenyl end groups), 5.54 (s, Ph−CH_2O−), 4.1 (s, −COO−CH_2−CH_2−), 3.57 (br, −Si−O−CH_3), 2.12 (br, −$CH_2C_7H_{15}$), 2.00 (s, $-C(CH_3)_2-$),1.25−1.10 (m, $-CH_2C_7H_{15}$), 0.83 (br, $-CH_2C(CH_3)(COO-)-$), 0.68 ($-CH_2-$Si−).

General Procedures for Micelle Preparation and Gelation. To prepare micelles, we dissolved PF-*b*-PMPS (1.0 mg) in THF (5.0 mL), and then a determinate amount of water was added dropwise by syringe at a rate of 1 drop every 10 s under vigorous stirring. The mixture was left stirring for an additional 12 h, and TEA (20 μL) was then added to induce the hydrolysis and polycondensation within micelles. The mixture was stirred for at least 72 h.

Results and Discussion

Synthesis and Characterization. The synthesis of monomers based on fluorene is widely reported.[20,21] The approaches

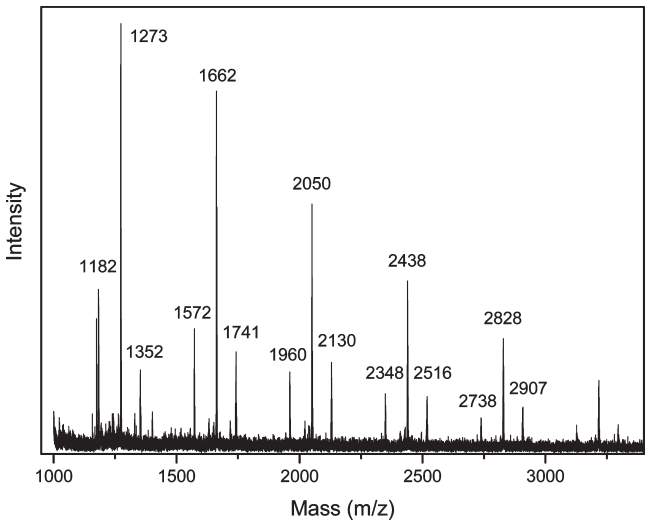

Figure 1. MALDI-TOF spectra of PFOH.

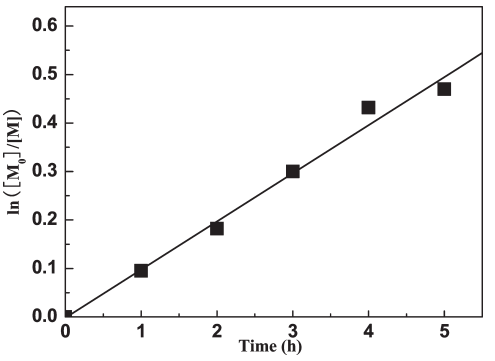

Figure 2. Kinetic plot for ATRP of MPS in *o*-dichlorobenzene initiated by PF macroinitiator with HMTETA/CuBr as the catalytic system ([HMTETA]/[CuCl]/[PF] = 2:2:1). V_{MPS}/V_{ODCB} = 1:60; 90 °C.

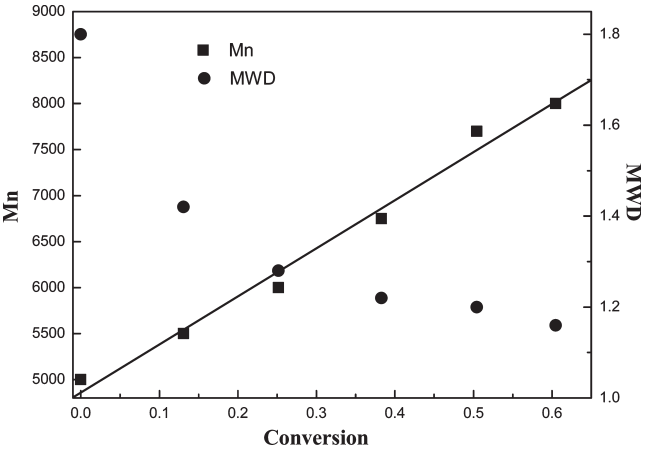

Figure 3. Dependence of molecular weight and molecular weight distribution (MWD) on monomer conversion for ATRP of MPS with PF with HMTETA/CuBr as the catalytic system ([HMTETA]/[CuCl]/[PF] = 2:2:1). V_{MPS}/V_{ODCB} = 1:60; 90 °C.

to alkylate and bromize the fluorene have been well studied and improved. The target product could be easily obtained with high yield and purity. However, there were some difficulties for the synthesis of 9,9-dioctyl-2-bromo-7-4,4,5,5-tetramethyl-1,3,2-dioxaborolan-2-yl fluorene because of the instability of boronate. Because of the unsymmetrical structure of 9,9-dioctyl-2-bromo-7-4,4,5,5-tetramethyl-1,3,2-dioxaborolan-2-yl, the product could not be purified via recrystallization as reported in the literature. Therefore, here we made the crude product pass through a long chromatographic column with petroleum ether as the eluent. The final product is a viscous and transparent liquid. The phenylboronic acid was synthesized according to the procedures reported in the literature.[22] The phenylboronic acid is very unstable so that the temperature must be kept as low as possible during the reaction and purification processes.

The Suzuki coupling reaction has proved to be very efficient in the polymerization of conjugated polymers.[20] Polyfluorene-based copolymers with two end-cappers could be synthesized through a one-pot Suzuki coupling reaction.[23] To offer enough solubility for the subsequent reaction, the molecular weight (Mn) of PF must be limited to a proper degree, and two end-capper monomers are added. 4-Bromobenzyl alcohol serves to functionalize the ends of the PF chains, and phenylboronic acid plays a role in controlling the polymerization degree.[18] To obtain more −OH-ended PF chains, we added 4-bromobenzyl alcohol after the Suzuki coupling reaction for 4 h, we added phenylboronic acid 4 h before the reaction completed. In fact, mono-ended PF chains with −OH are important for the subsequent reaction, and the benzene or −Br at the other end could not affect the next reaction.

By the addition of a determinate amount of these two end-capped monomers, the −OH-ended PF was obtained with the M_n of 5000 and M_w of 9000, indicating that each polymer chain contains about 10 fluorene units. Then, MALDI-TOF was used to analyze the proportions of end groups, and the spectra are shown in Figure 1. From calculation, it was found that more than 85% polymer chains were ended with 4-bromobenzyl alcohol, which was the vital functional group for the next synthesis step. 2-Bromoisobutyrate derivatives have been proven to be not only versatile for ATRP of many vinyl monomers[24] but also suitable for conjugated polymer.[17−19] Because of the high reaction activity, the esterification of PF with 2-bromoisobutyryl bromide was easy to carry out, even at room temperature. However, high temperature should be avoided during the concentration procedure because of the instability (and high reaction activity).

ATRP of MPS was conducted in ODCB solution with CuBr/HMTETA as the catalytic system. MPS is a highly reactive monomer and is very sensitive to the presence of water, especially under slightly basic or acidic conditions. Great caution must be paid to avoid possible gelation of the reaction mixture because of the sensitive trimethoxysilyl functions. The molecular weight of the block copolymer could be controlled by the amount of MPS added. In the case of polymerization, MPS was added by about 0.01, 0.02, 0.06 mmol separately, and thus three diblock polymers (**P1**−**P3**) were obtained with increasing number-average molecular weights of about 6000, 8600, and 14 000, which were determined by GPC.

Five samples were taken out from the reaction mixture of **P2** with 1 h interval. The molecular weight and molecular weight distribution (MWD) were determined by GPC, and the conversion was determined by ^{1}H NMR. A linear relationship was observed on the first-order kinetic plot (Figure 2), indicating the presence of a constant number of the growing species during the polymerization. The linear increase in the molecular weight and the narrow MWD of the resulting copolymers support the controlled fashion of the ATRP of MPS, as shown in Figure 3. Because the macroinitiator was obtained through a step-growth polymerization approach where the molecular weight is controlled by the ratio of the end-capper instead of the polymerization mechanism, the PF macroinitiator presented

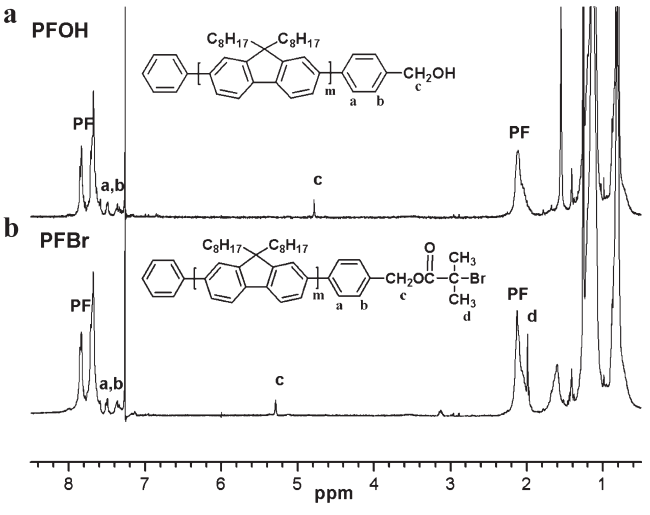

Figure 4. ^{1}H NMR spectra of PFOH and PF macroinitiators.

Table 1. MPS Monomer Added and the Molecular Weights of the PFOH and PF-*b*-PMPS from ^{1}H NMR and GPC

	MPS (μL/mmol)	Mn (^{1}H NMR)	Mn (GPC)	M_w (GPC)	M_w/M_n (GPC)
PFOH		5000	5000	9000	1.80
P1	2.5/0.01	6200	6000	8000	1.33
P2	5/0.02	8300	8600	10 000	1.16
P3	15/0.06	13 700	13 000	20 000	1.53

a poorly controlled MWD (M_w/M_n = 1.8). However, all of the copolymers obtained by ATRP showed a relatively narrow MWD (as listed in Table 1). Compared with the macroinitiator, the considerable decrease in MWD values for the block copolymers should be attributed to the well-defined PMS chains existing in the copolymers.[18]

The chemical structures of the PFOH, PFBr macroinitiators, and PF-*b*-PMPS block copolymers were confirmed by ^{1}H NMR. The ^{1}H NMR spectra of PFOH and PFBr macroinitiators are very consistent with the literature.[18] Here only the benzyl alcohol end-capper was paid much attention because the benzene end-capper at the other end was used only to combine the Br-ended fluorene chain. In fact, both benzene end-capper and Br end-capper did not affect the subsequent reactions much. The distinct peaks between 7.50 and 7.65 ppm in the spectra of PFOH and PFBr clearly showed the successful incorporation of the end-capping phenylene groups. The distinct peaks at δ = 4.78 in Figure 4a were assigned to Ph$-CH_2-$OC$=$O. Compared with the peaks at δ = 7.83, the proportions of peak integral areas indicated that there are about 10 fluorene units being connected with a benzyl alcohol capper per polymer chain, which was consistent with the result of GPC. The peaks at δ = 5.29 in Figure 4b were also assigned to Ph$-CH_2-$OC$=$O, which shifted to low field because of the presence of bromoisobutyryl. The absence of single resonance at δ = 4.78 in Figure 4b indicated a complete transformation of hydroxy into bromoisobutyrate functionality in the macroinitiator. The sharp peak at δ = 1.99 in Figure 4b was also convincing evidence of the bromoisobutyryl end-capper.

The ^{1}H NMR spectra of PF-*b*-PMPS (Figure 5) accorded with the literature.[7] The distinct peak at δ = 4.10 was assigned to COOCH_2 of the MPS, and the broad peaks at δ = 3.50 were assigned to methoxy of MPS. These spectra indicated that a long PMPS chain was connected to the PF macroinitiators, thus forming a diblock copolymer. From the integral area ratios of the peaks at about δ = 7.7 and 7.9 (which were assigned to the PF) and the peak at δ = 4.10 (which was assigned to COOCH_2 of MPS), the number of MPS units connected to PF macroinitiators could be calculated. The numbers of MPS units determined from ^{1}H NMR spectra were 5, 13, and 35, respectively, for **P1**, **P2**, and **P3**. These results were quite consistent with the GPC results.

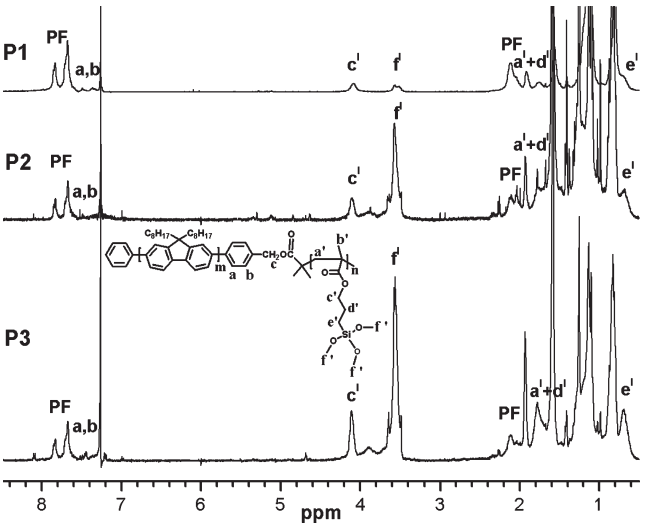

Figure 5. ^{1}H NMR spectra of PF-*b*-PMPS diblock copolymers.

PF homopolymer is soluble in THF, whereas PMPS homopolymer is water insoluble. And R$-$Si(OCH$_3$)$_3$ groups of PMPS may be easily hydrolyzed into $-$Si(OH)$_3$, which could be subsequently transferred into cross-linked polysilsesquioxane by polycondensation. As a result, in THF/aqueous solution, PF-*b*-PMPS block copolymers will be able to self-assemble into micelles with PMPS as the core and PF as the corona. Therefore, core$-$shell-type micelles can be spontaneously formed when water is added to THF solution of PF-*b*-PMPS block copolymers (in this work, at an initial concentration of 2 mg/mL). For the solubility in THF/water, we prepared only four water contents: 5, 10, 15, and 20% v/v for further research. We also had tried to get more samples from 5 to 50% v/v per 5%, but precipitation occurred and the mixtures became emulsifiable upon water contents of 20%. The nanospheres thus formed in mixed solution will undergo sol$-$gel processes upon the addition of a small amount of TEA by inducing chemical cross-linking of the PMPS core. A drop of such solution was taken out for TEM observation.

Figure 6 shows the TEM images of the hybrid micelles formed at water contents of 5 to 20% v/v (water/THF) for **P2**. It can be seen that these nanospheres have a regular spherical shape with a diameter of about 100$-$200 nm in the case of 5$-$15% water content. In general, the diameter slightly increases with increasing water content. (Not all of the nanospheres follow this rule because of the dispersivity of the copolymer.) It can be clearly observed that the micelles consist of core and shell nanostructures: the dark core is composed of high-density PMPS blocks, and the gray shell with thickness of about 30$-$40 nm is composed of PF blocks. When the water content increases to 20%, however, the nanospheres by TEM (Figure 6D) are different from those shown in Figure 6A$-$C. Some yellow deposits were observed in the reaction bottle when the water content rose to 20%. It is probably because too much water content is not favorable for the formation of core$-$shell nanospheres because of the limited solubility. Some polymer chains may be aggregated and deposited, and only a few polymer chains are left to form the nanospheres. This may induce the formation of a kind of vesicle structure with low density, as shown in gray contrast under TEM observation (Figure 6D). Therefore, the

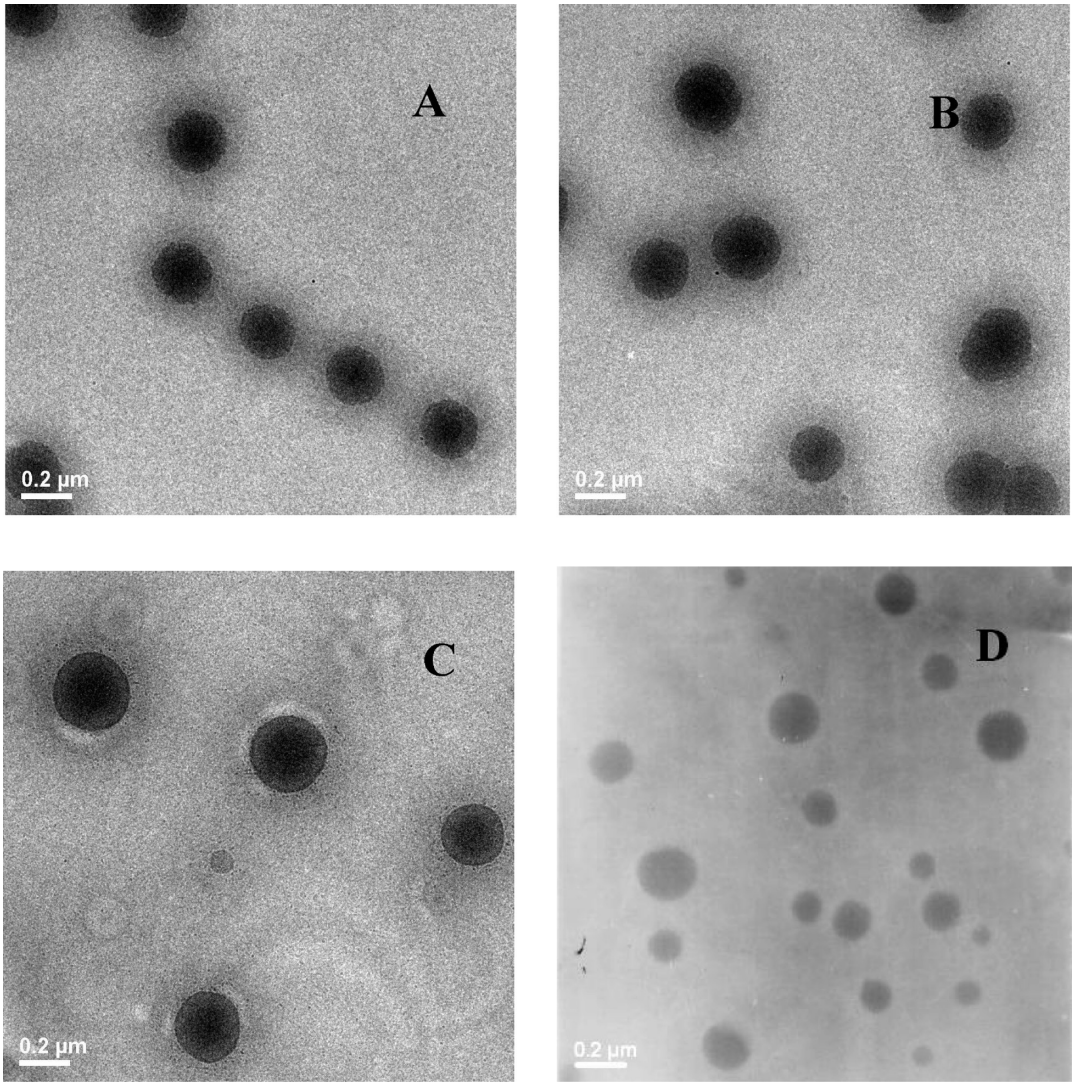

Figure 6. TEM images of the nanospheres prepared from PF-*b*-PMPS at different water content: (A) 5, (B) 10, (C) 15, and (D) 20% v/v.

Scheme 1. Schematic Illustration of the Synthesis Process and Structure of the Microspheres with PMPS As the Core and PF As the Corona

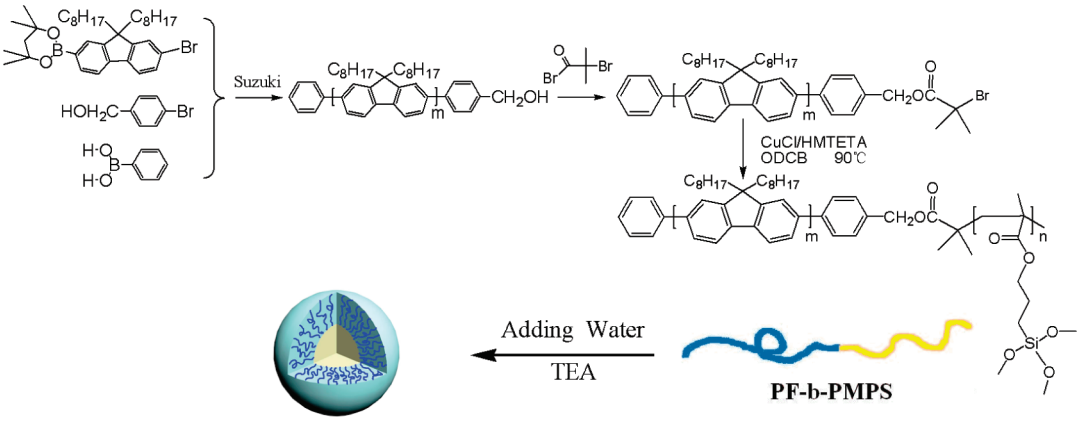

morphologies of the nanospheres are affected by the water content, and water is a very important factor for the hydrolyzation of trimethoxysilane groups, which is closely related to the formation of the PMPS core.

However, PF homopolymer shows limited solubility in water/THF solution. Therefore, here only four lower water contents, that is, 5, 10, 15, and 20% v/v were prepared for our study. Actually, more efforts have been made to prepare the solution samples with higher water content (above 20%); however, the precipitation occurred and the polymer solutions of water/THF became emulsifiable. In addition, all three samples (**P1**−**P3**) were used to attempt to prepare the micelles. However, only the **P2** sample thus prepared shows well-developed regular micelles under TEM observation. One can suppose that the micelle is built up by many polymer chains. If the PMS block is too short, then it will be difficult to

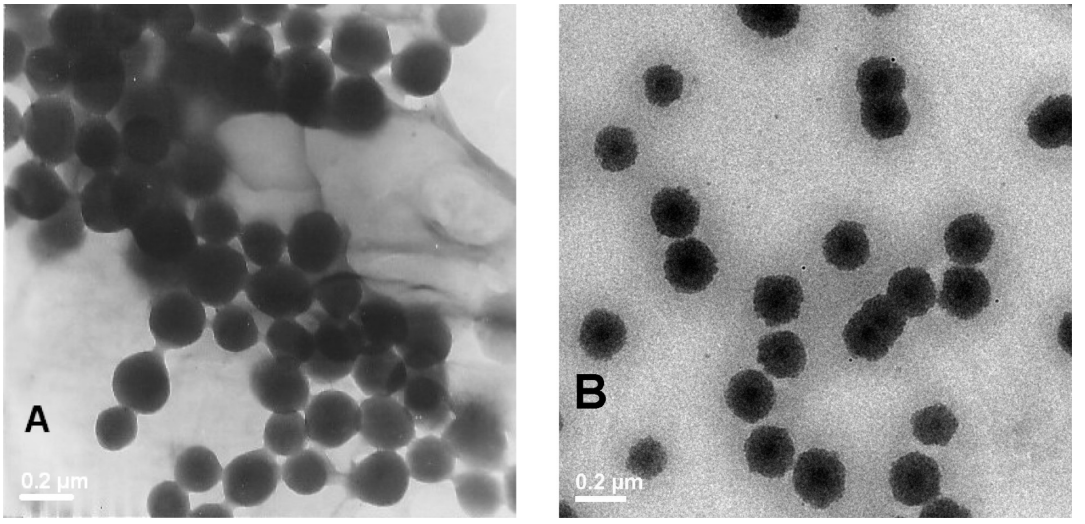

Figure 7. TEM images of the nanospheres prepared from PF-*b*-PMPS at 10% v/v water content: (A) 3 days after fabrication and (B) 30 days after fabrication and preserving without solution.

build up a polysilsesquioxane core; reversely, if the PMS block is too long, it may polycondensate by itself or just polycondensate with a limited number of polymer chains. The above two cases are not applicable to the formation of the micelles. Therefore, with a suitable chain length of PMS block, regular shape microspheres for **P2** were observed by TEM (as shown in Figure 6). A schematic illustration of the preparation and formation of hybrid core−shell micelles is shown in Scheme 1.

Moreover, the nanospheres thus prepared are quite stable because of the cross-linked core. Figure 7A,B shows the TEM images of the nanospheres prepared from PF-*b*-PMPS at 10% water content for 3 days and for 30 days after fabrication, respectively, by preserving without solution. It can be seen that the nanospheres being preserved without stirring in solution for 1 month were still almost the same as before. In fact, the nanospheres did not change much, even after the solvents were volatilized for 1 month (Figure 7B). Close inspection indicates that the freshly prepared nanospheres (Figure 7A) possess some pipelike structures connecting to each other, which may result in the aggregation formation of the nanospheres under certain conditions. After remaining at ambient for 1 month (without solvents), the nanospheres become surprisingly dispersible from each other, and the regular sphere shape is still preserved; whereas the pipelike linked structure disappears (Figure 7B).

Optical Properties. The UV−visible absorption and PL spectra were measured for the micelles solutions diluted in THF with the ratio of 1:4 (v/v), as shown in Figures 8 and 9. PF-*b*-PMPS copolymer was used as a reference to investigate the changes of optical property induced by the formation of the nanospheres. Generally speaking, the UV and PL spectra are very similar to those of PF homopolymer reported in the literature,[25] indicating that the nanospheres of PF-*b*-PMPS copolymer still keep the optical properties of PF.

The UV−visible absorption data of PF-*b*-PMPS diblock copolymers and the nanospheres with different water contents were shown in Figure 8. It can be seen that all have an absorption maximum at about 385 nm, which is the characteristic maximum absorption peak of PF. It is indicated that the ultraviolet absorption property of PF-*b*-PMPS diblock copolymers did not change much after the formation of nanospheres. It is known that the PMPS block (without aromatic structure) does not show any ultraviolet absorption within the studied range, and for the core−shell

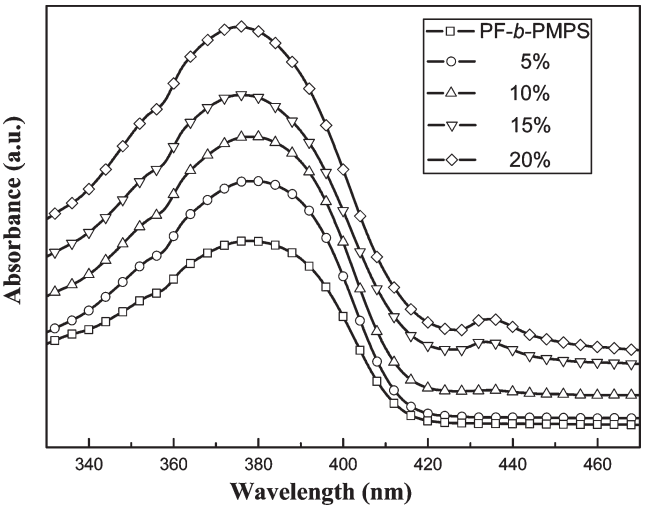

Figure 8. UV−vis absorption spectra of PF-*b*-PMPS diblock copolymers and the nanospheres at different water contents.

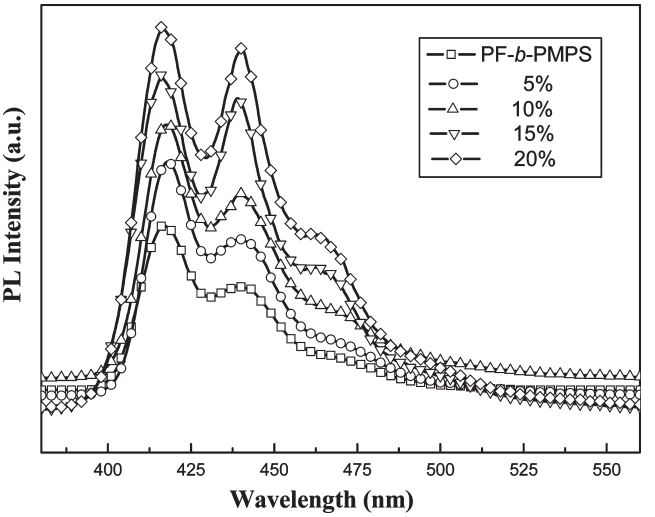

Figure 9. PL spectra of PF-*b*-PMPS diblock copolymers and the nanospheres at different water contents.

nanospheres, the polysilsesquioxane core is "coated" by the PF shell; as the result, the PF block will determine the whole ultraviolet absorption.

Figure 9 shows the PL spectra of PF-*b*-PMPS diblock copolymers and the nanospheres at different water contents. Some distinct changes were observed on PL spectra. PF has two characteristic maximum luminescence peaks at about 415 and 440 nm, respectively. The intensity of the peak at 415 nm is usually lower than that at 440 nm. The PL spectra of PF-*b*-PMPS copolymer does not show any difference from that of PF homopolymer, also indicating that the incorporation of PMPS block does not have an effect on the optical properties of the PF block. However, the spectra from the bottom to the top (with increasing the water content) showed a steady increase for the peak intensity at 440 nm. It indicated that the low-energy luminescence was gradually enhanced because of the formation of nanospheres. The PF blocks are usually very disordered in the solution of the PF-*b*-PMPS copolymer. However, upon the formation of the core−shell micelles in the water/THF solvent, the PF chains are arranged orderly (or in partially ordered fashion) and are compactly aggregated in the shell of the nanospheres. Such a difference in the spatial arrangement of polymer chains must cause the changes of PL spectra. It is supposed that the fluorene planes in the orderly arranged polymer chains are almost parallel and contiguous to each other. Therefore, the excimers could be easily formed under such circumstance and may cause the low-energy radiation. More ordered structure will be formed when more water is added to the PF-*b*-PMPS/THF solution, thus resulting in the increase in the peak intensity at 440 nm.

Electrochemical Properties. CV was employed to evaluate the ionization potentials and the redox stability of the conjugated polymers synthesized. Here PF-*b*-PMPS copolymer was also used as a reference to investigate the electrochemical property changes induced by the formation of the core−shell nanospheres. The CV was performed in a three-electrode cell with a solution of Bu_4NPF_6 (0.1 M) in acetonitrile at a scan rate of 50 mV/s at room temperature under the protection of argon. A glass carbon electrode was coated with a thin polymer film and used as the working electrode. A Pt wire was used as the counter electrode, and the $Ag/AgNO_3$ reference electrode was used as the reference electrode. The onset potentials are determined from the intersection of the two tangents drawn at the rising current and the baseline charging current of the CV traces.[26] The oxidation and reduction potentials were used to estimate the highest occupied molecular orbital (HOMO) and the lowest unoccupied molecular orbital (LUMO) energy levels. Therefore, the HOMO and LUMO levels were calculated according to the following empirical formula

$$E_{HOMO} = -(E_{ox} + 4.4)\ \text{eV}\ (\text{Ag/Ag}^+)$$

$$E_{LOMO} = -(E_{re} + 4.4)\ \text{eV}\ (\text{Ag/Ag}^+)$$

The curves of the oxidation process were shown in Figure 10, and the data were listed in Table 2. The UV−vis band gap is deduced from optical absorption spectra of ultraviolet spectra and also listed in Table 2 for comparison. It can be seen that the band gaps (E_g) obtained by CV measurements were larger than those estimated from UV−vis data. This phenomenon is widely reported in the literature.[26] The difference may be caused by the interface barrier between the polymer film and the electrode surface. The electrochemical data may be the combination of the optical band gap and the interface barrier for charge injection, thus making them larger. However, the UV−vis data do not account for exciton binding energy. As a result, there exists such a difference between the data obtained by the two methods. Moreover, the solution mixture is a disturbance system, which is completely different from the solid film. The spatial arrangement of the polymer chains does not have much effect on this system. Therefore, no distinct change was found for the five samples.

Additionally, the data from CV measurements showed an interesting dual characteristic. The homopolyfluorene usually shows HOMO energy level of about −5.50 eV and LUMO energy level of about −2.4 eV.[21] Here the HOMO energy level of PF-*b*-PMPS copolymer is about −5.4 eV, which is close to the data reported in the literature for PF homopolymer. However, the LUMO energy level of PF-*b*-PMPS copolymer is about −1.2 eV, which is far away from the data reported in the literature for PF homopolymer. However, it should be noted that the LUMO energy level of polysilanes was reported to be about −1.2 eV,[27] which is very close to the data obtained in the present study. Therefore, we supposed that the oxidation and reduction processes of the PF-*b*-PMPS diblock copolymer are probably dominated by two blocks, respectively: the oxidation

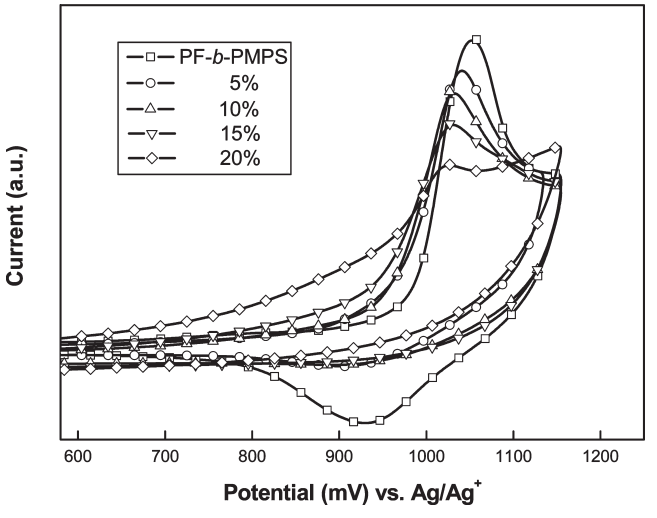

Figure 10. Cyclic voltammograms of PF-*b*-PMPS diblock copolymers and the nanospheres coated on platinum plate electrodes in acetonitrile containing 0.10 M Bu_4NBF_4. Platinum wire is used as the counter electrode. The potentials reference against Ag/0.10 M $AgNO_3$ in acetonitrile. Scan rate: 50 mV/s.

Table 2. Electrochemical Properties of the PF-*b*-PMPS Diblock Copolymers and the Nanospheres Determined from Absorption Onset and CV Data

	λ_{abs} (onset) (nm)	UV−vis band gap (eV)	cyclic voltammetry				
			$E_{onset/ox}$ (V)	$E_{onset/red}$ (V)	HOMO (eV)	LUMO (eV)	band gap (eV)
PF-*b*-PMPS	405.98	3.07	0.98	−3.27	−5.38	−1.13	4.25
5%	407.20	3.06	0.96	−3.18	−5.36	−1.22	4.14
10%	406.80	3.07	0.95	−3.18	−5.35	−1.22	4.13
15%	404.94	3.08	0.93	−3.18	−5.33	−1.22	4.11
20%	405.57	3.08	0.91	−3.19	−5.32	−1.21	4.11

process is dominated by PF block and the reduction process is dominated by PMPS block. A light decrease was found for the HOMO energy data for the four core−shell nanosphere systems. This was probably due to the changes in spatial arrangement for the polymer chains upon the formation of core−shell nanostructure, thus leading to the formation of excimers. No distinct change was found for the LUMO energy level for the four nanosphere systems, probably because this is dominated by PMPS core. And compared with the PF-*b*-PMPS copolymer, a distinct gap could also be found because the spatial arrangement of polymer chains was changed after the formation of the cores.

Conclusions

A new approach for preparing luminescent core−shell nanospheres has been developed in this article. In THF/aqueous solution, amphiphilic PF-*b*-PMPS diblock copolymers can self-assemble into micelles with PMPS core and PF shell. The base-catalyzed sol−gel process inside the PMPS core induces the formation of PF-encapsulated silica core−shell nanospheres. Without any heavy metal chromophores, these nanospheres show high shape stability and have blue-light-emitting feature with high efficiency because of excellent PL property of the PF block itself. The influence of the nanospheres formation on the optical and electrochemical properties of the PF-*b*-PMPS diblock copolymers is investigated in detail. These luminescent nanospheres may find potential applications in bioanalysis, biomedical, and light-emitting devices.

Acknowledgment. This work was financially supported by the National Natural Science Foundation of China (50403012, 20704009), the "Program for New Century Excellent Talents in University" (NCET-04-035), the "Shanghai Rising-Star Program" (04QMX1403), the Program for Changjiang Scholars and Innovative Research Team in University (PCSIRT) (IRT0612), and the Shanghai Leading Academic Discipline Project (B113).

References and Notes

(1) Alivisatos, A. P. *Science* **1996**, *271*, 933.
(2) Du, J.; Chen, Y. *Macromolecules* **2004**, *37*, 6322.
(3) Daniel, M. C.; Astruc, D. *Chem. Rev.* **2004**, *104*, 293–346.
(4) Du, J.; Chen, Y.; Zhang, Y.; Han, C. C.; Fischer, K.; Schmidt, M. *J. Am. Chem. Soc.* **2003**, *125*, 14710.
(5) Du, J.; Chen, Y. *Macromolecules* **2004**, *37*, 5710.
(6) Du, J.; Chen, Y. *Macromol. Rapid Commun.* **2005**, *26*, 491.
(7) Zhang, Y.; Luo, S.; Liu, S. *Macromolecules* **2005**, *38*, 9813–9820.
(8) Zhang, H.; Cui, Z.; Wang, Y.; Zhang, K.; Ji, X.; Liu, C.; Yang, B.; Gao, M. *Adv. Mater.* **2003**, *15*, 777.
(9) Wolcott, A.; Gerion, D.; Visconte, M.; Sun, J.; Schwartzberg, A.; Chen, S.; Zhang, J. Z. *J. Phys. Chem. B* **2006**, *110*, 5779–5789.
(10) Skaff, H.; Ilker, M. F.; Coughlin, E. B.; Emrick, T. *J. Am. Chem. Soc.* **2002**, *124*, 5729.
(11) Yang, Y.; Gao, M. *Adv. Mater.* **2005**, *17*, 2354.
(12) Zhelev, Z.; Ohba, H.; Bakalova, R. *J. Am. Chem. Soc.* **2006**, *128*, 6324.
(13) Chan, Y.; Zimmer, J. P.; Stroh, M.; Steckel, J. S.; Jain, R. K.; Bawendi, M. G. *Adv. Mater.* **2004**, *16*, 2092.
(14) Mamedov, A. A.; Belov, A.; Giersig, M.; Mamedova, N. N.; Kotov, N. A. *J. Am. Chem. Soc.* **2001**, *123*, 7738.
(15) Heeger, A. J. *Solid State Commun.* **1998**, *107*, 673.
(16) Grice, A. W.; Bradley, D. D. C.; Bernius, M. T.; Indasekaran, M.; Wu, W. W.; Woo, E. P. *Appl. Phys. Lett.* **1998**, *73*, 629.
(17) Lu, S.; Fan, Q. L.; Liu, S. Y.; Chua, S. J.; Huang, W. *Macromolecules* **2002**, *35*, 9875–9881.
(18) Lu, S.; Fan, Q. L.; Liu, S. Y.; Huang, W. *Macromolecules* **2003**, *36*, 304–310.
(19) Lu, S.; Liu, T. X.; Ke, L.; Ma, D. G.; Chua, S. J.; Huang, W. *Macromolecules* **2005**, *38*, 8494.
(20) Ranger, M.; Rondeau, D.; Leclerc, M. *Macromolecules* **1997**, *30*, 7686–7691.
(21) Liu, B.; Yu, W. L.; Lai, Y. H.; Huang, W. *Chem. Mater.* **2001**, *13*, 1984–1991.
(22) Jensen, M. P.; Lange, S. J.; Mehn, M. P.; Que, E. L.; Que, L. *J. Am. Chem. Soc.* **2003**, *125*, 2113.
(23) Schmitt, C.; Nothofer, H. G.; Falcou, A.; Scherf, U. *Macromol. Rapid Commun.* **2001**, *22*, 624.
(24) Matyjaszewski, K.; Xia, J. *Chem. Rev.* **2001**, *101*, 2921.
(25) Yang, G. Z.; Wang, W. Z.; Wang, M.; Liu, T. X. *J. Phys. Chem. B* **2007**, *111*, 7747.
(26) Chen, Z. K.; Huang, W.; Wang, L. H.; Kang, E. T.; Chen, B. J.; Lee, C. S.; Lee, S. T. *Macromolecules* **2000**, *33*, 9015.
(27) Wang, W. Z.; Fan, Q. L.; Cheng, F.; Zhao, P.; Huang, W. *J. Polym. Sci., Part A: Polym. Chem.* **2006**, *44*, 3513.